Electronic Supplementary Information

Green light enhanced the photostability and catalytic performance of fatty acid photodecarboxylase

Ao Xia,*[ab] Xiaobo Guo,[ab] Yingxin Chai,[ab] Wuyuan Zhang,[cd] Yun Huang,[ab] Xianqing Zhu,[ab] Xun Zhu[ab] and Qiang Liao*[ab]

[a] *Key Laboratory of Low-grade Energy Utilization Technologies and Systems, Chongqing University, Ministry of Education, Chongqing 400044, China*

[b] *Institute of Engineering Thermophysics, School of Energy and Power Engineering, Chongqing University, Chongqing 400044, China*

[c] *Tianjin Institute of Industrial Biotechnology, Chinese Academy of Sciences, Tianjin 300308, China*

[d] *National Center of Technology Innovation for Synthetic Biology, Tianjin 300308, China*

* Corresponding authors: aoxia@cqu.edu.cn (Ao Xia); lqzx@cqu.edu.cn (Qiang Liao).

Tel: +86 23 65106832; Fax: +86 23 65102474.

1. Materials

All chemicals and reagents were purchased from Sangon Biotech or Aladdin. They were used without further purification unless otherwise noted.

2. Influence of blue and green light on *Cv*FAP catalysis

2.1 Detection of light spectrum characteristics

The photocatalytic system used in this study is shown in Fig. S1. The light sources were adjusted to blue, green, and red light, respectively. Then, the light spectrum was identified by the QE65000 spectrometer (Ocean Optics Co.).

2.2 Catalytic condition of *Cv*FAP

The broken cells catalyst (*Cv*FAP BCs) was prepared from the recombinant *Escherichia coli* containing *Cv*FAP after supersonic treatment, which was used as *Cv*FAP catalyst in this work.[1,2] Photoenzymatic decarboxylation was conducted under aerobic and anaerobic environments with blue, green, and red light as light sources, respectively. The typical conditions of photoenzymatic decarboxylation were as the following: The reaction mixture included 500 μL of Tris-HCl buffer (pH 8.5, 100 mM), 300 μL of DMSO as a cosolvent containing 40 mM palmitic acid, and 200 μL of *Cv*FAP (with an initial cell dry weight of 140.8 mg/mL) in a 5 mL transparent glass vial. The initial concentration of palmitic acid in the catalytic system was 12 mM. Regarding anaerobic decarboxylation, the reaction vial was deoxygenized in an anaerobic workstation (Concept 400; Ruskinn Technology, UK) and sealed.[2] Deoxygenization

was not performed for aerobic decarboxylation. The decarboxylation reaction was triggered by the illumination of a Light Emitting Diode (LED) light source (light intensity of 200 $\mu mol \cdot m^{-2} \cdot s^{-1}$) and stirring at 200 rpm and 30 °C for 1 h. The pentadecane yield was detected according to our previous work.[1]

To further improve the catalytic efficiency of *Cv*FAP under green light illumination, the influence of catalytic time (i.e., 30, 60, 120, and 150 min) on the pentadecane yield was investigated following the aforementioned typical conditions.

3. Influence of blue and green light on the catalytic stability of *Cv*FAP

The influences of blue and green light on photoenzymatic decarboxylation at both a low *Cv*FAP concentration and a high substrate concentration were conducted to investigate the catalytic stability of *Cv*FAP under aerobic and anaerobic environments. The catalytic condition followed the aforementioned typical conditions, except for using 100 μL of *Cv*FAP and 54 mM of palmitic acid.

The reactive oxygen species (ROS) in the catalytic system of *Cv*FAP under an aerobic environment were assessed with electron paramagnetic resonance (EPR) to explore the influence mechanism of the blue and green light on the catalytic stability of *Cv*FAP according to our previous work.[2]

4. Influence of blue and green light preillumination on *Cv*FAP catalysis

Since *Cv*FAP is readily suppressed in the blue light preillumination with substrate absent.[2-4] The influences of blue and green light preillumination on *Cv*FAP catalysis

under aerobic and anaerobic environments were investigated. In blue light preillumination under aerobic and anaerobic environments, a 5 mL transparent glass vial containing 500 μL of Tris-HCl buffer (pH 8.5, 100 mM) and 200 μL of *Cv*FAP was preilluminated at 200 μmol·m^{-2}·s^{-1} of blue light, 200 rpm, and 30 °C for various time (*i.e.*, 10, 20, 40, and 60 min). Subsequently, to assess the residual activity of *Cv*FAP, 300 μL of DMSO cosolvent containing 40 mM palmitic acid was supplemented in the transparent glass vial to initiate the photoenzymatic decarboxylation for 2 h. Identically, the green light preillumination followed the aforementioned procedure using green light instead of blue light. The ratio of pentadecane yield after preillumination to pentadecane yield without preillumination represented the residual activity of *Cv*FAP.

Since almost no ROS was generated in the preillumination system under an anaerobic environment,[2] the production of ROS in the preillumination system under an aerobic environment was assessed with EPR to further explore the influence mechanism of the blue and green light preillumination on *Cv*FAP catalysis according to our previous work.[2]

5. Influence of blue and green light on photodegradation kinetics of flavin adenine dinucleotide

Flavin adenine dinucleotide (FAD) is the key site of *Cv*FAP to capture photons, and its photostability plays a vital role in the catalytic stability of *Cv*FAP.[5-7] The absorption spectrums of FAD under blue and green light illumination were detected with an ultraviolet-visible spectrophotometer. Due to different degradation rates of FAD under

blue light and green light illumination, 50 μM of FAD in Tris-HCl buffer (pH 8.5, 100 mM) was illuminated by blue light and green light for various time, in terms of 0, 1, 4, 8, 12, 16, 20, 32, 40, and 48 min for blue light, and 0, 60, 120, 180, 240, 300, 360, 420, and 480 min for green light. The time courses of A_{450} of FAD under blue light and green light illumination were recorded, which were also fitted with quasi-first order kinetic model as shown in Eq. (1).[8]

$$\ln \frac{(C_t)}{C_0} = -kt \tag{1}$$

where C_0 is the initial A_{450} of FAD. C_t is the A_{450} of FAD at time t (min). k is the degradation rate constant of FAD (min^{-1}).

6. Influence of blue and green light on the reaction kinetics of *Cv*FAP

To investigate the influence mechanism of blue and green light on *Cv*FAP activity, the Michaelis-Menten equation (Eq. (2)) was employed to obtain the kinetic characteristics of *Cv*FAP catalysis under blue light illumination and green light illumination. To obtain the initial reaction rate, photoenzymatic decarboxylation with various concentration of palmitic acid at 12, 18, 24, and 30 mM were conducted for 5, 10, 15, and 20 min, where the catalytic system consisted of 100 μL *Cv*FAP, 600 μL Tris-HCl buffer (pH 8.5, 100 mM), and different concentrations of palmitic acid in 300 μL DMSO. The catalytic condition followed the typical decarboxylation condition in Section 2.2. The apparent Michaelis constant (K_m) and the maximum reaction rate (V_{max}) of *Cv*FAP catalysis under blue light illumination and green light illumination were obtained from the Lineweaver-Burk plot as shown in Eq. (3).

5

$$v = \frac{V_{max}[S]}{K_m + [S]} \qquad (2)$$

$$\frac{1}{v} = \frac{K_m}{V_{max}} \cdot \frac{1}{[S]} + \frac{1}{V_{max}} \qquad (3)$$

where v is the reaction rate at time t, and [S] is the concentration of palmitic acid at time

t.

7. Influence of blue and green light on the reaction thermodynamics of CvFAP

The thermodynamic characteristics of CvFAP catalysis help to illustrate the influence mechanism of the blue and green light on the CvFAP activity. To obtain the reaction rate constant of CvFAP at different temperatures (10, 15, 20, and 25 °C), the catalytic system consisting of 100 μL CvFAP, 600 μL Tris-HCl buffer (pH 8.5, 100 mM), and 40 mM of palmitic acid in 300 μL DMSO was employed. The catalytic condition followed the typical decarboxylation condition in Section 2.2, where the reaction time were 5, 10, 15, and 20 min. As the photoenzymatic decarboxylation followed a first-order kinetic reaction equation at 12 mM of palmitic acid, the reaction rate constant could be obtained according to Eqs. (4) and (5).

$$\frac{d(S)}{dt} = k(S) \qquad (4)$$

$$\ln\frac{(S_t)}{S_0} = kt \qquad (5)$$

where S represents the concentration of palmitic acid. S_0 and S_t are the concentration of palmitic acid at time 0 and t, respectively.

The activation energy of CvFAP is obtained according to the Arrhenius equation as shown in Eq. (6).

$$k = Ae^{-E_a/RT} \tag{6}$$

where Arrhenius constant A and E_a are the frequency factor (min^{-1}) and activation energy (J/mol). R is the molar gas constant (8.314 J mol^{-1} K^{-1}). T is the degree kelvin (K). Eq. (7) can be obtained by taking the natural logarithm of Eq. (6).

$$\ln k = \ln A - \frac{E_a}{RT} \tag{7}$$

The ΔG can be ontained according to the Eyring-Polanyi equation of Eq. (8).

$$k = \frac{k_b T}{h} \exp(-\frac{\Delta G}{RT}) \tag{8}$$

By taking the natural logarithm of Eq. (8) and substituting $\Delta G = \Delta H - T\Delta S$, Eq. (9) can be obtained.

$$\ln(\frac{k}{T}) = -(\frac{\Delta H}{RT}) + \left[\ln K + \ln(\frac{k_b}{h}) + \frac{\Delta S}{R} \right] \tag{9}$$

where ΔH and ΔS are the enthalpy change of activation and entropy change of activation, respectively. k is the rate constant (min^{-1}). T is the degree Kelvin (K). R, k_b, and h are the molar gas constant (8.314 J mol^{-1} K^{-1}), Boltzmann constant (1.38×10^{-23} J/K), and Planck constant (6.63×10^{-34} J S), respectively. K is the mass transfer coefficient.
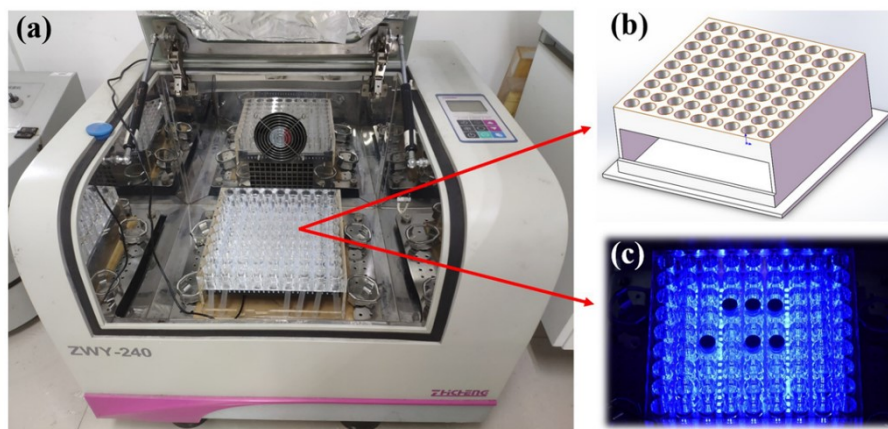
Fig. S1 Image of homemade photocatalytic system. (a) Image of the reactor. (b) Diagram of the catalytic unit. (c) Image of the catalytic unit.
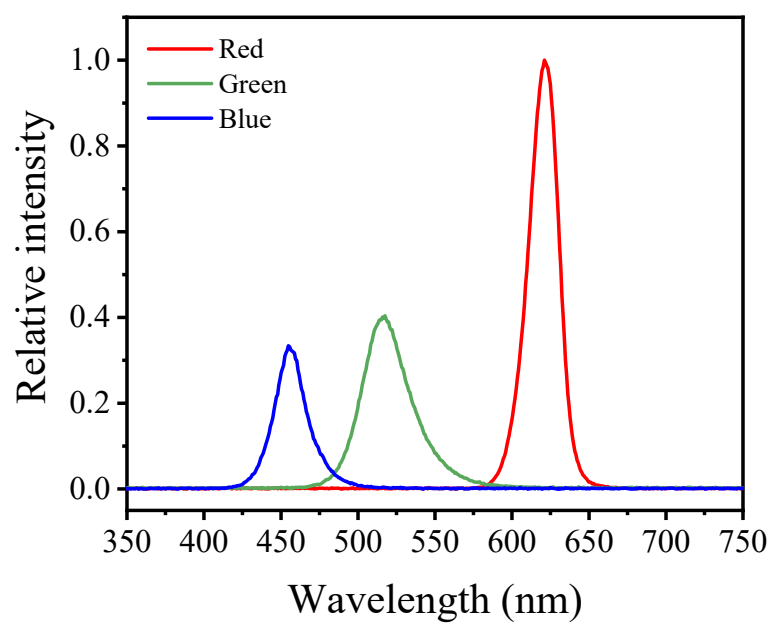
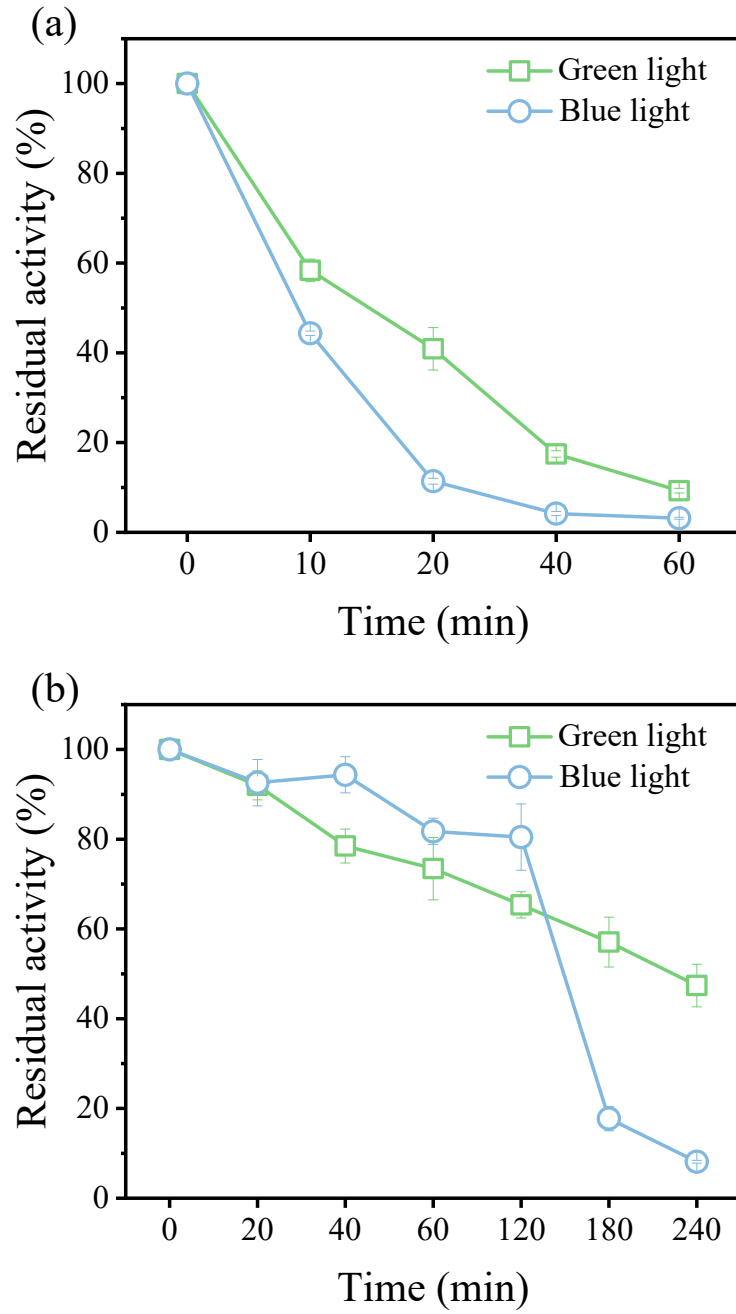**Fig. S2** The light spectrum of the light sources.

Fig. S3 Influence of blue and green light preillumination on the residual activity of *Cv*FAP. (a) Preillumination under an aerobic environment. (b) Preillumination under an anaerobic environment.
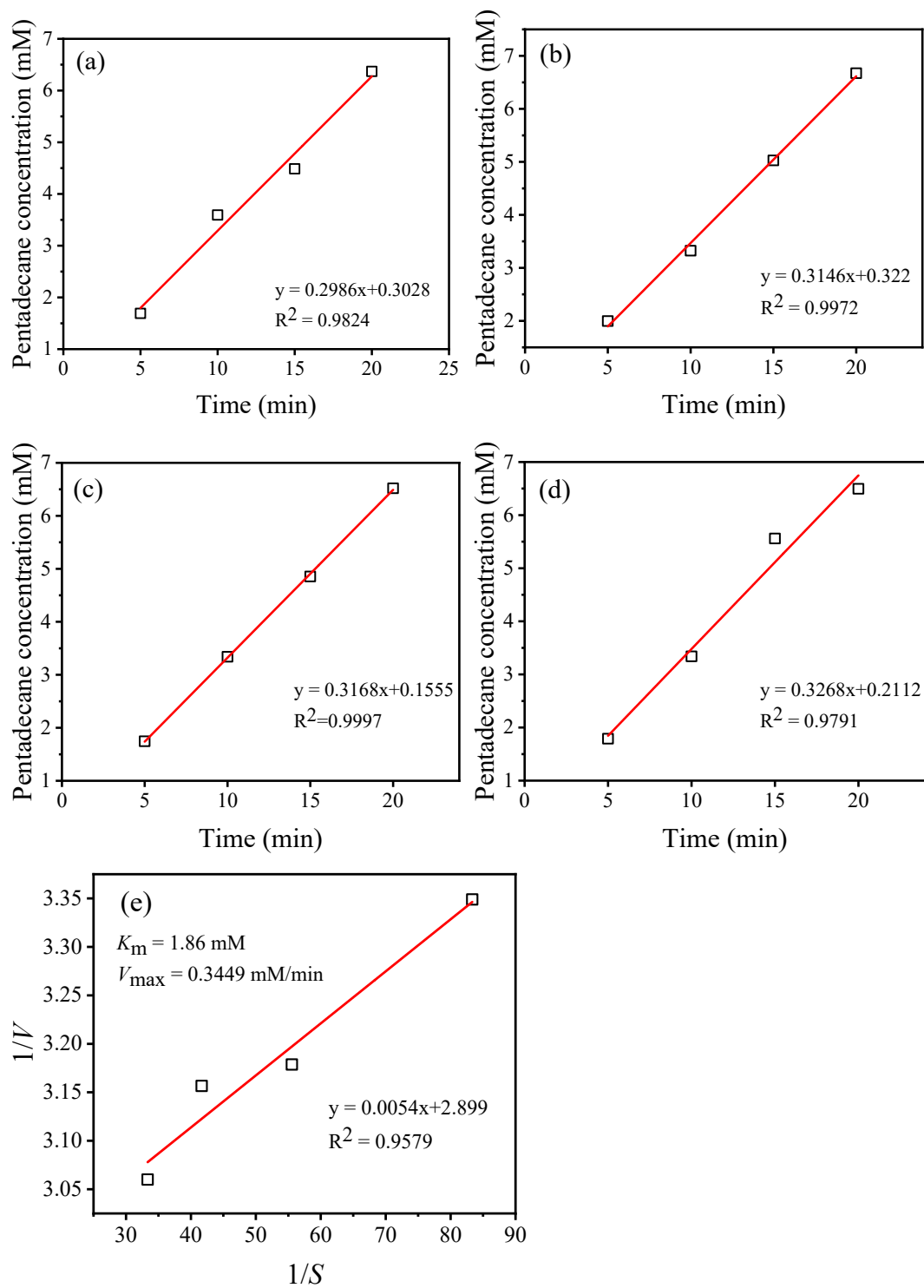
Fig. S4 Kinetics analysis of *Cv*FAP catalysis under blue light illumination. Initial substrate concentrations in (a)-(d) are 12, 18, 24, and 30 mM, respectively. (e) Lineweaver-Burk plot.
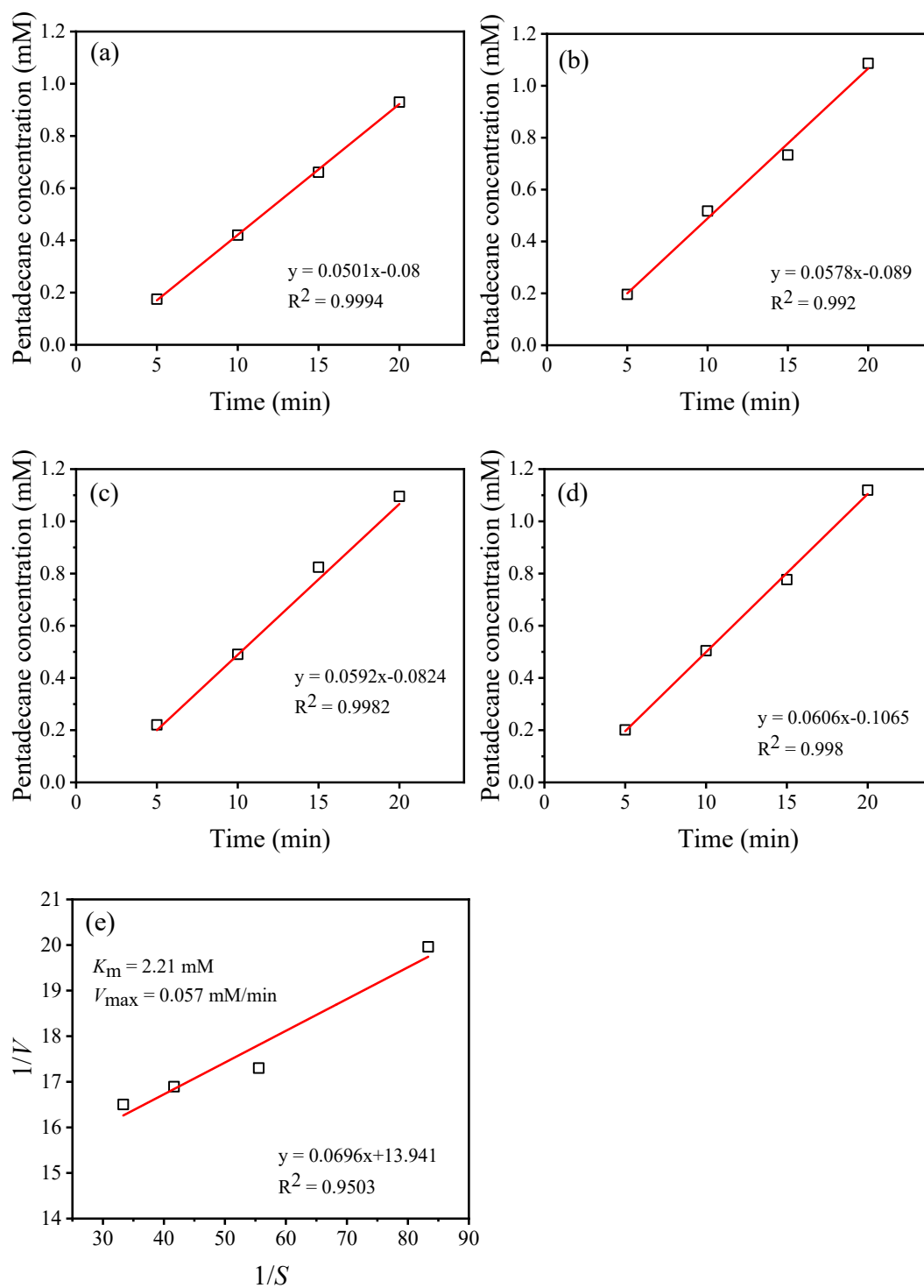
Fig. S5 Kinetics analysis of *Cv*FAP catalysis under green light illumination. Initial substrate concentrations in (a)-(d) are 12, 18, 24, and 30 mM, respectively. (e) Lineweaver-Burk plot.
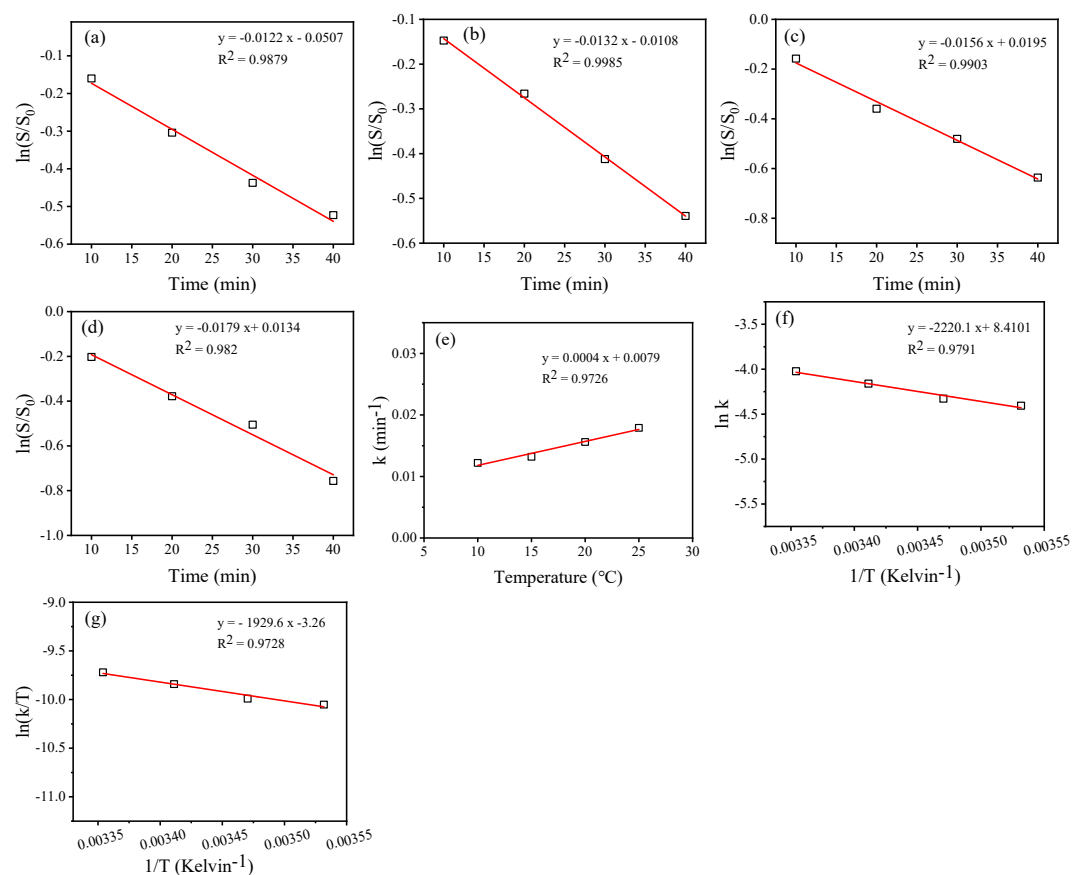
Fig. S6 Thermodynamic characteristics of *Cv*FAP catalysis under blue light illumination. *Cv*FAP catalysis processes in (a)-(d) are at 10, 15, 20, and 25 °C, respectively. (e) Plots of rate constant *vs.* temperature. (f) Arrhenius plot of ln*k vs* 1/*T*. (g) Eyring plot of ln*k*/*T vs.* 1/*T*.
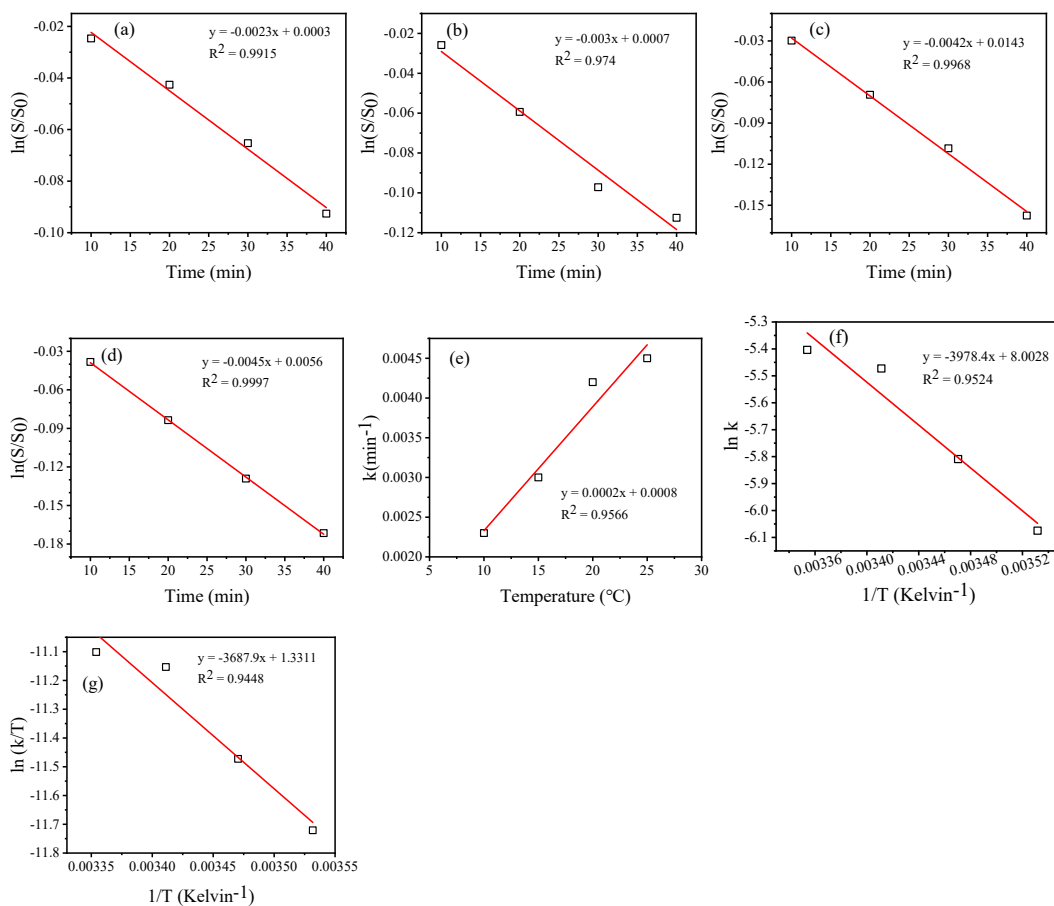
Fig. S7 Thermodynamic characteristics of *Cv*FAP catalysis under green light illumination. *Cv*FAP catalysis processes in (a)-(d) are at 10, 15, 20, and 25 °C, respectively. (e) Plots of rate constant *vs.* temperature. (f) Arrhenius plot of ln*k vs* 1/*T*. (g) Eyring plot of ln*k*/*T vs.* 1/*T*.

Table S1 The light spectrum characteristics of different light sources.

Light source	Peak wavelength	Half-peak breadth
Blue LED	454	22
Green LED	518	35
Red LED	621	22

LED: Light Emitting Diode.

Table S2 Thermodynamic characteristics of *Cv*FAP catalysis.

Light sources	E_a (kJ/mol)	A (min^{-1})	ΔH (kJ/mol)
Blue light	18.456	4492.2	16.043
Green light	33.076	2989.3	30.661

E_a: Activation energy; A: Frequency factor; ΔH: Enthalpy change of activation.

References

1 X. Guo, A. Xia, F. Li, Y. Huang, X. Zhu, W. Zhang, X. Zhu and Q. Liao. *Energy Conv. Manag.*, 2022, **255**, 115311.

2 X. Guo, A. Xia, W. Zhang, F. Li, Y. Huang, X. Zhu, X. Zhu and Q. Liao. *Chin. Chem. Lett.*, 2022, **34**, 107875.

3 M. M. E. Huijbers, W. Zhang, F. Tonin and F. Hollmann. *Angew. Chem.-Int. Edit.*, 2018, **57**, 13648-13651.

4 Y. Wu, C. E. Paul and F. Hollmann. *ChemBioChem*, 2021, **22**, 2420-2423.

5 D. Sorigue, B. Legeret, S. Cuine, S. Blangy, S. Moulin, E. Billon, P. Richaud, S. Brugiere, Y. Coute, D. Nurizzo, P. Mueller, K. Brettel, D. Pignol, P. Arnoux, Y. Li-Beisson, G. Peltier and F. Beisson. *Science*, 2017, **357**, 903-907.

6 D. J. Heyes, B. Lakavath, S. J. O. Hardman, M. Sakuma, T. M. Hedison and N. S. Scrutton. *ACS Catal.*, 2020, **10**, 6691-6696.

7 D. Sorigue, K. Hadjidemetriou, S. Blangy, G. Gotthard, A. Bonvalet, N. Coquelle, P. Samire, A. Aleksandrov, L. Antonucci, A. Benachir, S. Boutet, M. Byrdin, M. Cammarata, S. Carbajo, S. Cuine, R. B. Doak, L. Foucar, A. Gorel, M. Grunbein, E. Hartmann, R. Hienerwadel, M. Hilpert, M. Kloos, T. J. Lane, B. Legeret, P. Legrand, Y. Li-Beisson, S. L. Y. Moulin, D. Nurizzo, G. Peltier, G. Schiro, R. L. Shoeman, M. Sliwa, X. Solinas, B. Zhuang, T. R. M. Barends, J. P. Colletier, M. Joffre, A. Royant, C. Berthomieu, M. Weik, T. Domratcheva, K. Brettel, M. H. Vos, I. Schlichting, P. Arnoux, P. Mueller and F. Beisson. *Science*, 2021, **372**, 148-159.

8 C. K. Remucal and K. McNeill. *Environ. Sci. Technol.*, 2011, **45**, 5230-5237.